Configuring Electronic States in an Atomically Precise Array of Quantum Boxes

Sylwia Nowakowska,[*] Aneliia Wäckerlin, Ignacio Piquero-Zulaica, Jan Nowakowski, Shigeki Kawai, Christian Wäckerlin, Manfred Matena, Thomas Nijs, Shadi Fatayer, Olha Popova, Aisha Ahsan, S. Fatameh Mousavi, Toni Ivas, Ernst Meyer, Meike Stöhr, J. Enrique Ortega, Jonas Björk, Lutz H. Gade,[*] Jorge Lobo-Checa,[*] Thomas A. Jung[*]

S. Nowakowska, Dr. A. Wäckerlin, Dr. S. Kawai, Dr. M. Matena, T. Nijs, S. Fatayer, O. Popova, A. Ahsan, S. F. Mousavi, Dr. T. Ivas, Prof. E. Meyer
Department of Physics, University of Basel, Klingelbergstrasse 82, 4056 Basel, Switzerland.
E-mail: sylwia.nowakowska@unibas.ch
I. Piquero-Zulaica, Prof. J. E. Ortega
Centro de Física de Materiales (CSIC/UPV-EHU) - Materials Physics Center, Manuel Lardizabal 5, 20018 San Sebastián, Spain.
J. Nowakowski, Dr. C. Wäckerlin, Prof. T. A. Jung
Laboratory for Micro- and Nanotechnology, Paul Scherrer Institute, 5232 Villigen PSI, Switzerland.
E-mail: thomas.jung@psi.ch
Dr. S. Kawai
PRESTO, Japan Science and Technology Agency (JST), 4-1-8 Honcho, Kawaguchi, Saitama 332-0012, Japan.
Dr. M. Matena, Prof. J. E. Ortega
Donostia International Physics Center (DIPC), Manuel Lardizabal 4, 20018 San Sebastián, Spain.
S. Fatayer
Departamento de Física Aplicada, Instituto de Física Gleb Wataghin, Universidade Estadual de Campinas, Campinas 13083-859, Brazil.
Prof. M. Stöhr
Zernike Institute for Advanced Materials, University of Groningen, Nijenborgh 4, 9747 AG Groningen, The Netherlands.
Prof. J. E. Ortega
Departamento Física Aplicada I, Universidad del País Vasco, 20018 San Sebastián, Spain.
Dr. J. Björk
Department of Physics, Chemistry and Biology, IFM, Linköping University, Linköping 581 83, Sweden.
Prof. L. H. Gade
Anorganisch-Chemisches Institut, Universität Heidelberg, Im Neuenheimer Feld 270, 69120 Heidelberg, Germany.
E-mail: lutz.gade@uni-hd.de
Prof. J. Lobo-Checa
Instituto de Ciencia de Materiales de Aragón (ICMA), CSIC-Universidad de Zaragoza, E-50009 Zaragoza, Spain.
Departamento de Física de la Materia Condensada, Universidad de Zaragoza, E-50009 Zaragoza, Spain.
E-mail: jorge.lobo@csic.es

Keywords: quantum box, electron confinement, surface state, scanning tunneling spectroscopy (STS), angle-resolved photoemission spectroscopy (ARPES)

We demonstrate that quantum states contained in quantum boxes, which are embedded in an ordered array, can be configured via their patterning with adsorbates. The quantum array is fabricated by on-surface self-assembly with ultimately high precision, which concerns the individual quantum box, the periodicity of the array and the coupling with the surrounding units. As an adsorbate we use Xe, whose occupancy we control by scanning tunneling microscope repositioning: each quantum box exhibits 12 filling levels, which incrementally perturb the quantum box state(s) via Pauli repulsion. We also show that the inter-box coupling can be sustained or significantly weakened by an appropriate arrangement of empty and filled boxes. Owing to complementary scanning tunneling microscopy/spectroscopy and angle-resolved photoemission spectroscopy studies we gain unprecedented insight into the physics of interacting quantum states on the local level as well as in their cooperative interaction. Our approach demonstrates that such self-assembled two-dimensional quantum box architectures may serve as nanoscale analog of breadboards commonly employed in electronic circuitry.

The development of quantum architectures, aimed to be employed e.g. in sensors and information technologies, relies upon the detailed understanding of the cooperative interaction of the unit systems involved. Towards this end, exploratory device architectures may be based on well-defined interacting units of limited complexity assembled in highly ordered arrays. Implementations of this concept include optical lattices generated by laser beam interference and microfabricated ion trap chips.[1,2] Whereas the former approach benefits from the strict periodicity of the interference pattern, the addressability of the unit components remains a challenge.[3] In contrast, in the latter case the traps can be controlled individually but the reliability of their fabrication is limited by the accuracy of the top-down micro/nanofabrication techniques employed.

On-surface quantum units exhibit discrete electronic states originating from the confinement of electrons in structures of different sizes and shapes.[4–13] Using scanning tunneling microscopy (STM) repositioning, well-defined quantum systems have been created. [7,8,14–16] More recently, these have been manufactured in the form of chains of atoms or vacancies in a self-assembled island to assess how their interaction depends on the unit size and arrangement.[17,18] Our approach goes beyond this concept in that we can configure the electronic states contained in quantum boxes (QBs) within extended 2D arrays by directed perturbation. The self-assembly approach allows for the manufacturing of identical QBs which are coupled in an inherently precise way,[4] and are addressable by targeted filling with an adsorbate which specifically perturbs, and thus modifies, the quantum box state (QBS). In particular, by changing the adsorbate occupancy via STM repositioning the energy levels of the QBSs and their coupling are modulated.

The array of coupled QBs employed in this work is based on a highly stable Cu-coordinated triply dehydrogenated 4,9-diaminoperylene quinone-3,10-diimine (3deh-DPDI) network generated on Cu(111) (**Figure 1**),[19–21] the pores of which partially confine the Shockley surface state of the underlying substrate.[4] In this system each pore contains a partially localized electronic ground state, while the n=2 state is practically lying at the Fermi energy (see Section 1 of Supporting Information).[4] The low intensity of the latter state and the absence of higher order bound states simplify the analysis of the targeted perturbation of the ground state by adsorbates and by its interaction with surrounding QBs. To modify the QBS in these pores we chose Xe atoms, for their well-defined interaction with the surface state electrons of Cu(111), which is dominated by Pauli repulsion,[22,23] and for its preferential adsorption in the pores of the Cu-coordinated 3deh-DPDI network with the maximal

occupancy of 12 atoms,[24] which offers the opportunity to discretely modify the electronic state in each QB by STM repositioning.

In our studies we characterize the 2D array of QBs by scanning tunneling microscopy/spectroscopy (STM/STS) providing site specific, *local* information on the effect of Xe adsorption on the QBS and by complementary angle-resolved photoemission spectroscopy (ARPES) giving access to the coherent, *ensemble*, part of the interaction between the partially localized states.

In the following we characterize two extreme network states: the vacant network and the fully filled network with 12 Xe atoms adsorbed in each QB to study the corresponding QBSs. The corresponding STM/STS and ARPES data are presented in Figure 1a-b and **Figure 2**, respectively. The emergence of an electronic band registered by ARPES in both cases (Figure 2) provides evidence for the partial localization and thus for the coupling between the QBSs.[4] The spatially resolved dI/dV trace in Figure 1a illustrates the spectral and spatial distribution of the partially localized state within the vacant network, whose maximum is observed at 201±6 meV Binding Energy (*BE*). Upon adsorption of 12 Xe atoms in each pore of the network, an additional, dominating, Xe induced localized component at lower *BE* appeared, whose maximum is observed at 136±7 meV (Figure 1b white arrow). This Xe related component is superimposed on the signal coming from partial localization of the QBS. The shift towards lower *BE* of the latter component upon Xe adsorption, as measured by ARPES, amounts to ~30 meV (**Table 1**). We interpret this energy shift as the result of Pauli repulsion between the electronic states of Xe and the QBS, similar to the previously reported shift of the Shockley surface state of bare Cu(111) towards lower *BE* caused by the adsorption of Xe (Table 1).[23] Notably, our results demonstrate that there is an apparent increase of the electron effective mass upon the filling of the network pores with Xe (Table 1, **Figure 3**).

This contrast with the case of the free-electron-like Cu(111) Shockley state, where no significant change of the effective mass is observed with an adsorbed Xe layer (cf. Table 1).[23] In the present case, we speculate that the extra increase of the effective mass in the network upon Xe pore filling is related to a weaker inter-pore coupling, *i.e.* to a change in the 2D network potential. A detailed theoretical study is under way to address this issue.

To investigate whether the filling of the surrounding QBs influenced the electronic state in a chosen unit, we generated different configurations by repositioning single Xe atoms with the STM tip.[25–27] Two model arrangements were studied in detail: a filled QB surrounded by empty ones (Figure 1c) and an empty QB surrounded by filled ones (Figure 1d).

In the first model case (Figure 1c), the spatially resolved dI/dV trace of the QBS for the filled pore is significantly different from the one observed for the individual pore in the Xe filled network (cf. Figure 1b): the Xe induced component at lower *BE* dominates (Figure 1c, white arrow), whereas the signal at higher *BE* originating from the electronic band created by the surrounding empty network is strongly attenuated: a sharp QBS peak with a full width at half maximum (FWHM) of ~50 meV is observed (Figure 1c, blue dI/dV spectrum). We attribute this sharpening to the additional out-of-plane confinement of the state via the Pauli repulsion imposed by Xe. The electronic coupling between electronic states depends on the electronic overlap which is reduced by the sharpening of the QBS of the filled QB and the state energy mismatch between the filled QB and the surrounding empty QBs, which feature the same spatially resolved dI/dV trace as the vacant array (cf. Figure 1a). Closer inspection reveals that the single filled pore exhibits a QBS peak at slightly higher *BE* than the filled network (Section 3 of Supporting Information, cf. Figure 1b). We tentatively attribute this to 2nd order coupling of this state to higher energy virtual states.

In the second model case of the central empty QB surrounded by filled ones (Figure 1d), the spatially resolved d*I*/d*V* trace of the QBS of the empty pore does not exhibit the Xe induced localization. Consequently the overlap between the electronic state of the empty QB and the electronic states of the surrounding filled QBs is not reduced (cf. Figure 1c). The d*I*/d*V* trace of the surrounding QBs is the same as for the filled network reference (Figure 1b), while the maximum of the QBS of the empty pore is observed at higher BE (247 ± 7) meV compared to the reference case of the vacant network (cf. Figure 1a). This energy shift can be explained within the framework of first order perturbation theory: the interaction of electronic states of one quantum system with states of neighboring quantum systems leads to the stabilization of the state of higher *BE* and the destabilization of one of the states of lower *BE* in its direct vicinity. For symmetry reasons the QBS of the empty pore will interact with the totally symmetric combination of the QBSs of the six adjacent filled pores leaving the other neighboring QBSs unaffected.[28] This, along with the broad QBS' d*I*/d*V* signatures limiting the spectral resolution, explains why we are not able to detect any change in the neigbouring filled QBs.

So far we discussed different network configurations comprising empty and fully filled QBs. To explore a broader spectrum of configurations we investigated the influence of partial Xe occupancy of the QB on the electronic state. Specifically, Xe atoms were removed step by step from an initially filled QB surrounded by an array of filled ones using STM repositioning. After each step a d*I*/d*V* spectrum was acquired. **Figure 4** summarizes the d*I*/d*V* spectra acquired for the prepared occupancies. Upon decrease of the Xe occupancy, the QBS peak energy is observed to gradually shift to higher *BE* until reaching 247±7 meV for an empty QB (Figure 4 red spectra). Such tuning of the QBS is also achieved for a similar series, in which the surrounding pores are empty (**Figure 5**).

In summary, we have demonstrated that controlling the Xe occupancy of each pore in 12 steps configures a self-assembled array of quantum boxes: the Pauli repulsion imposed by Xe atom(s) modifies the quantum box states and, notably, adds an additional confining dimension to the coupled quantum boxes. Therefore our work demonstrates that the simplified picture of the emergence of the confined states from the 2D electron gas needs to be extended to include potential confinement effects in the out-of-plane dimension and underpins the well-established fact that the observed physical effects at interfaces are not by nature strictly 2D. Moreover, we would like to point out that there are similarities between our discussion of the coupling in artificial QB systems and the interatomic interactions in molecular physics. Our approach opens up the possibility to use a combination of various adsorbates in order to create more complex experimentally addressable patterns of quantum states, well beyond the scope of this paper.

Experimental Section

Sample preparation for STM/STS measurements: The Cu-coordinated 3deh-DPDI network on Cu(111) was prepared according to the procedure described in Ref. [20]. Xe of purity 99.99% was dosed onto the sample placed in the STM (Omicron Nanotechnology GmbH with Nanonis SPM control system) operated at 4.2 K, with the cryoshields open and the leak valve being in line-of-sight with the sample. The sample was exposed to 120 L (Langmuir) of Xe (1.3×10^{-7} mbar for 1200 s) resulting in the increase of the sample temperature to 9 K. The STM measurements performed after cooling the sample back to 4.2 K revealed different numbers of Xe atoms adsorbed in the pores as well as at the domain boundaries and step edges. Filling of all pores with 12 Xe atoms was performed by subsequent annealing to 45 K followed by cooling to 4.2 K for the STM measurements.

Repositioning of single Xe atoms: All the condensates discussed in the manuscript were obtained by controllable removing of Xe atoms from the pores of the network by means of STM repositioning. Noticeably, new configurations that are not occurring spontaneously upon Xe exposure can be created in this way (*i.e.* occ-4, occ-6b and occ-8b, cf. Figure 3 and Ref. [24]).

STM/STS measurement details and data analysis: In the STM the bias voltage is applied to the tip. The bias voltages given in the manuscript and the SI refer to a grounded tip.
STM measurements were performed in constant current mode with Pt-Ir tips (90% Pt, 10% Ir), prepared by mechanical cutting followed by sputtering and controlled indentation in the bare Cu(111) substrate. All STM images were acquired with a Xe functionalized tip, which allows for obtaining atomic resolution on Xe condensates.[24]
To avoid modification of the condensates via interaction with the tip, the sample bias was selected within a range of -10 mV – -80 mV, whereas the tunnelling current was set within the range of 5 pA – 50 pA. The exact tunneling parameters for the STM images presented in the main text are displayed in Table S1.
The STM data were processed with the WSxM software.[29] For better comparability of the data the color histograms of the STM images were adjusted. Low-pass filtering was used for noise reduction.
All dI/dV spectra were recorded with open-feedback loop and with Xe functionalized tip. Control spectra were acquired with a metallic tip and no difference was observed in accordance with Ref. [30].
The dI/dV data presented in Figure 1 are extracted from the grid spectroscopy measurements, in which area of 7.8 nm x 4.3 nm was mapped by acquisition of dI/dV spectra above each point with the resolution of 50 points x 30 points for the empty network and 60 points x 30 points for the other three cases. The initial tip conditions amounted to 400 mV/70 pA (lock-in

frequency: 513 Hz; zero-to-peak amplitude: 8 mV). As described in detail in Ref. [31] the value of the initial voltage was chosen such, that no quantum box state or network backbone related contribution was present. Owing to that a normalization could be performed by setting the same dI/dV value at the setpoint energy for all dI/dV spectra. In this way artefacts originating from local work function variations are minimized.

The dI/dV spectra presented in Figure 4 and Figure 5 were acquired with the initial tip conditions amounting to -800 mV/50 pA (lock-in frequency: 513 Hz; zero-to-peak amplitude: 5 mV).

ARPES setup: The ARPES measurements were performed on a lab-based experimental setup equipped with a display type hemispherical analyser (Phoibos150) with an energy/angle resolution of 40 meV / 0.1º and a monochromatized Helium I ($h\nu$=21.2 eV) source.

Sample preparation and ARPES acquisition details: To avoid contributions from the Shockley surface state of bare Cu(111) to the ARPES signal, it was crucial to achieve a homogeneous Cu-coordinated 3deh-DPDI network completely covering the surface. Therefore, DPDI was sublimed onto Cu(111) held at room temperature in wedge geometry (coverage gradient) in the proximity of the optimal coverage and then annealed until a sharp and intense signal emerging from partial localization of the quantum box state, as in Ref. [4], was visible in the ARPES channelplate detector. The annealing step is crucial for conversion of the DPDI molecules into 3deh-DPDI molecules, which create the Cu-coordinated network.[20,21] The Xe dosing experiment was started immediately after the sample temperature dropped below 60 K, but was higher than 25 K to keep the adsorbate mobility.[32] Xe core level (9 to 5 eV *BE*) and surface state (close to Fermi energy) regions at normal emission were acquired alternatively as a function of time while keeping Xe pressure in the chamber constant (5×10^{-10} mbar). The evolution of the $5p_{3/2}$ and $5p_{1/2}$ core levels and partially

localized part of the quantum box state as function of the Xe exposure time is shown in Figure S1 (total exposure time amounted to ~30 min).

Supporting Information

Supporting Information is available from the Wiley Online Library or from the author.

Acknowledgements

We would like to acknowledge the financial support from the Swiss Nanoscience Institute (SNI), Swiss National Science Foundation (grants No. 200020-149713, 206021-121461), the Spanish Ministry of Economy (grant No. MAT2013-46593-C6-4-P), the Basque Government (grant No. IT621-13), the São Paulo Research Foundation (grant #2013/04855-0), Swiss Government Excellence Scholarship Program, Netherlands Organization for Scientific Research NWO (Chemical Sciences, VIDI-grant No. 700.10.424) the European Research Council (ERC-2012-StG 307760-SURFPRO), University of Basel, University of Heidelberg, Linköping University, University of Groningen, Paul Scherrer Institute, and the Japan Science and Technology Agency (JST) `Precursory Research for Embryonic Science and Technology (PRESTO)' for a project of `Molecular technology and creation of new function'. We sincerely thank Marco Martina and Rémy Pawlak for the support during measurements.

Received: ((will be filled in by the editorial staff))
Revised: ((will be filled in by the editorial staff))
Published online: ((will be filled in by the editorial staff))

[1] I. Bloch, *Nat. Phys.* **2005**, *1*, 23.
[2] T. D. Ladd, F. Jelezko, R. Laflamme, Y. Nakamura, C. Monroe, J. L. O'Brien, *Nature* **2010**, *464*, 45.
[3] I. Buluta, F. Nori, *Science* **2009**, *326*, 108.
[4] J. Lobo-Checa, M. Matena, K. Müller, J. H. Dil, F. Meier, L. H. Gade, T. A. Jung, M. Stöhr, *Science* **2009**, *325*, 300.
[5] F. Klappenberger, D. Kühne, W. Krenner, I. Silanes, A. Arnau, F. J. García de Abajo, S. Klyatskaya, M. Ruben, J. V. Barth, *Nano Lett.* **2009**, *9*, 3509.
[6] F. Klappenberger, D. Kühne, W. Krenner, I. Silanes, A. Arnau, F. J. García de Abajo, S. Klyatskaya, M. Ruben, J. V. Barth, *Phys. Rev. Lett.* **2011**, *106*, 026802.
[7] M. F. Crommie, C. P. Lutz, D. M. Eigler, *Science* **1993**, *262*, 218.
[8] E. J. Heller, M. F. Crommie, C. P. Lutz, D. M. Eigler, *Nature* **1994**, *369*, 464.
[9] P. Avouris, I.-W. Lyo, *Science* **1994**, *264*, 942.
[10] N. Nilius, T. M. Wallis, W. Ho, *Science* **2002**, *297*, 1853.
[11] Y. Pennec, W. Auwärter, A. Schiffrin, A. Weber-Bargioni, A. Riemann, J. V. Barth, *Nat. Nanotechnol.* **2007**, *2*, 99.
[12] S. Wang, W. Wang, L. Z. Tan, X. G. Li, Z. Shi, G. Kuang, P. N. Liu, S. G. Louie, N. Lin, *Phys. Rev. B* **2013**, *88*, 245430.
[13] A. Shchyrba, S. C. Martens, C. Wäckerlin, M. Matena, T. Ivas, H. Wadepohl, M. Stöhr, T. A. Jung, L. H. Gade, *Chem. Commun.* **2014**, *50*, 7628.
[14] J. Repp, G. Meyer, S. Paavilainen, F. E. Olsson, M. Persson, *Science* **2006**, *312*, 1196.

[15] F. Mohn, J. Repp, L. Gross, G. Meyer, M. Dyer, M. Persson, *Phys. Rev. Lett.* **2010**, *105*, 266102.
[16] C. Krull, R. Robles, A. Mugarza, P. Gambardella, *Nat. Mater.* **2013**, *12*, 337.
[17] K. Seufert, W. Auwärter, F. J. García de Abajo, D. Ecija, S. Vijayaraghavan, S. Joshi, J. V. Barth, *Nano Lett.* **2013**, *13*, 6130.
[18] S. Fölsch, J. Martínez-Blanco, J. Yang, K. Kanisawa, S. C. Erwin, *Nat. Nanotechnol.* **2014**, *9*, 505.
[19] M. Stöhr, M. Wahl, C. H. Galka, T. Riehm, T. A. Jung, L. H. Gade, *Angew. Chem. Int. Ed.* **2005**, *44*, 7394.
[20] A. Shchyrba, C. Wäckerlin, J. Nowakowski, S. Nowakowska, J. Björk, S. Fatayer, J. Girovsky, T. Nijs, S. C. Martens, A. Kleibert, M. Stöhr, N. Ballav, T. A. Jung, L. H. Gade, *J. Am. Chem. Soc.* **2014**, *136*, 9355.
[21] M. Matena, J. Björk, M. Wahl, T.-L. Lee, J. Zegenhagen, L. H. Gade, T. A. Jung, M. Persson, M. Stöhr, *Phys. Rev. B* **2014**, *90*, 125408.
[22] J.-Y. Park, U. Ham, S.-J. Kahng, Y. Kuk, K. Miyake, K. Hata, H. Shigekawa, *Phys. Rev. B* **2000**, *62*, R16341.
[23] F. Forster, S. Hüfner, F. Reinert, *J. Phys. Chem. B* **2004**, *108*, 14692.
[24] S. Nowakowska, A. Wäckerlin, S. Kawai, T. Ivas, J. Nowakowski, S. Fatayer, C. Wäckerlin, T. Nijs, E. Meyer, J. Björk, M. Stöhr, L. H. Gade, T. A. Jung, *Nat. Commun.* **2015**, *6*, 6071.
[25] D. M. Eigler, C. P. Lutz, W. E. Rudge, *Nature* **1991**, *352*, 600.
[26] A. Yazdani, D. M. Eigler, N. D. Lang, *Science* **1996**, *272*, 1921.
[27] G. Kichin, C. Weiss, C. Wagner, F. S. Tautz, R. Temirov, *J. Am. Chem. Soc.* **2011**, *133*, 16847.
[28] E. Merzbacher, *Quantum Mechanics*, Wiley, New York, **1970**.
[29] I. Horcas, R. Fernández, J. M. Gómez-Rodríguez, J. Colchero, J. Gómez-Herrero, A. M. Baro, *Rev. Sci. Instrum.* **2007**, *78*, 013705.
[30] H. C. Manoharan, C. P. Lutz, D. M. Eigler, *Nature* **2000**, *403*, 512.
[31] W. Krenner, D. Kühne, F. Klappenberger, J. V. Barth, *Sci. Rep.* **2013**, *3*, 1454.
[32] J.-Y. Park, S.-J. Kahng, U. Ham, Y. Kuk, K. Miyake, K. Hata, H. Shigekawa, *Phys. Rev. B* **1999**, *60*, 16934.

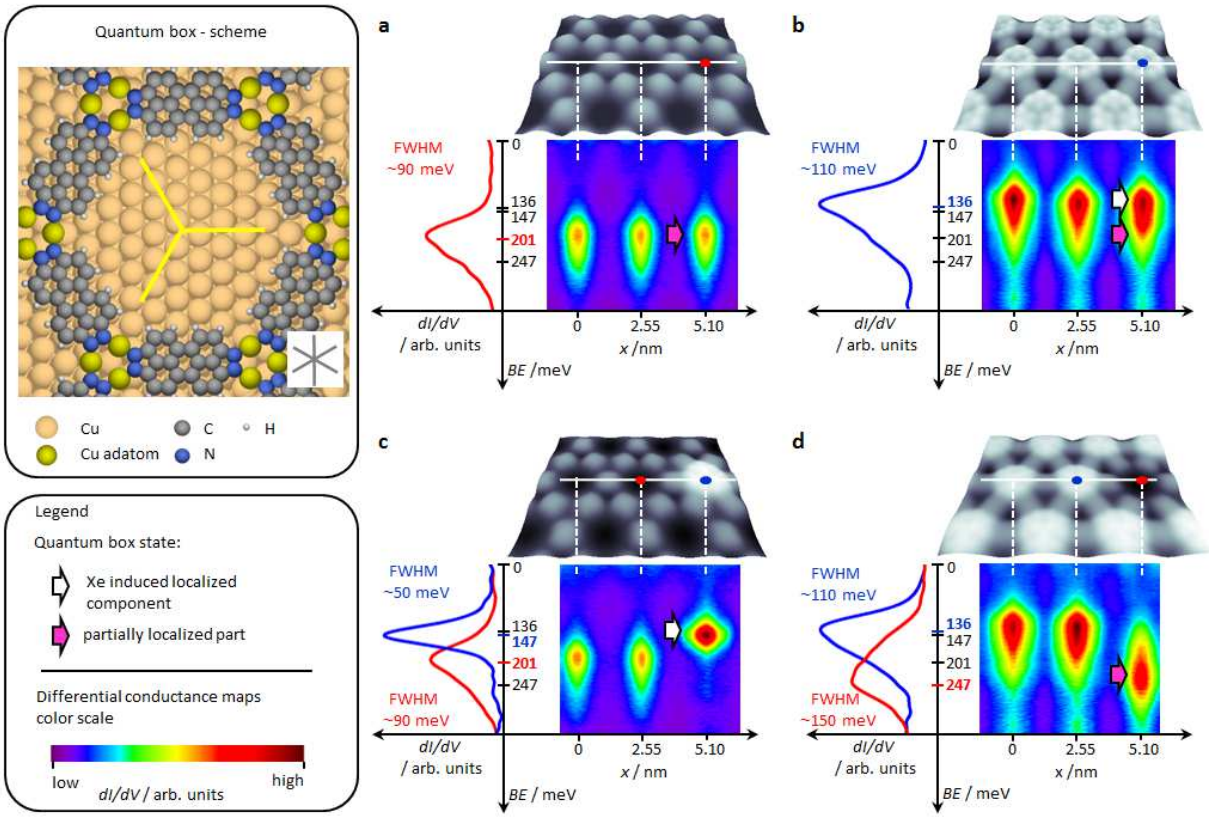

Figure 1. Xe patterning of quantum boxes. (upper inset) Schematic representation of a pore of Cu-coordinated 3deh-DPDI network constituting a quantum box. The quantum box states contained in the pores of the on-surface network are modified by Xe atoms deposition and their subsequent removal by STM repositioning sequences. The d*I*/d*V* spectra reflect the spectral distribution of the quantum box state for each configuration. Right hand side: four different network configurations for investigating cooperative interactions between the quantum box states: (a) empty network, (b) filled network with 12 Xe atoms adsorbed in each box, (c) filled quantum box with 12 Xe atoms surrounded by empty boxes and (d) empty quantum box surrounded by filled quantum boxes with 12 Xe atoms adsorbed in each box. In each case, a series of d*I*/d*V* spectra was acquired along the white line (indicated in the STM images) crossing three quantum boxes. The spectra are visualized as spatially resolved d*I*/d*V* traces. The d*I*/d*V* spectra taken at the red and blue colored dots superimposed on the STM images are plotted on the left hand side of the d*I*/d*V* traces (size of STM images 7.8 nm x 4.3 nm).

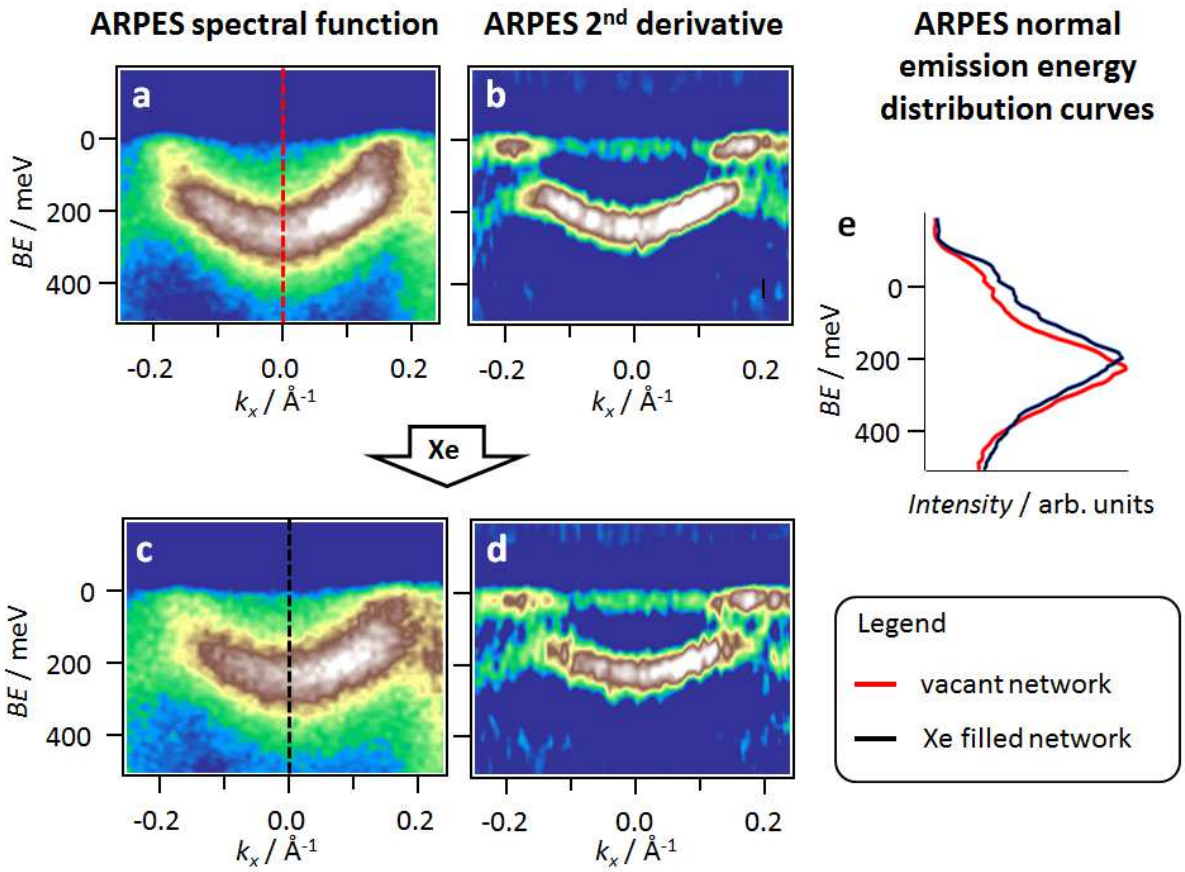

Figure 2. Influence of Xe adsorption on the coherent (*ensemble*) interaction between the partially localized parts of the quantum state hosted by the pores of the network. (a) ARPES experimental spectral function acquired for the empty network and (b) its second derivative measured along the $\bar{\Gamma}\ \bar{M}$ high symmetry direction. (c) ARPES experimental spectral function after Xe adsorption in the pores and (d) its second derivative. (e) Normal emission energy distribution curves (k_x=0) from a and c. The spectra acquired between these two cases are shown in Figure S1, Supporting Information (cf. Section 2 of Supporting Information).

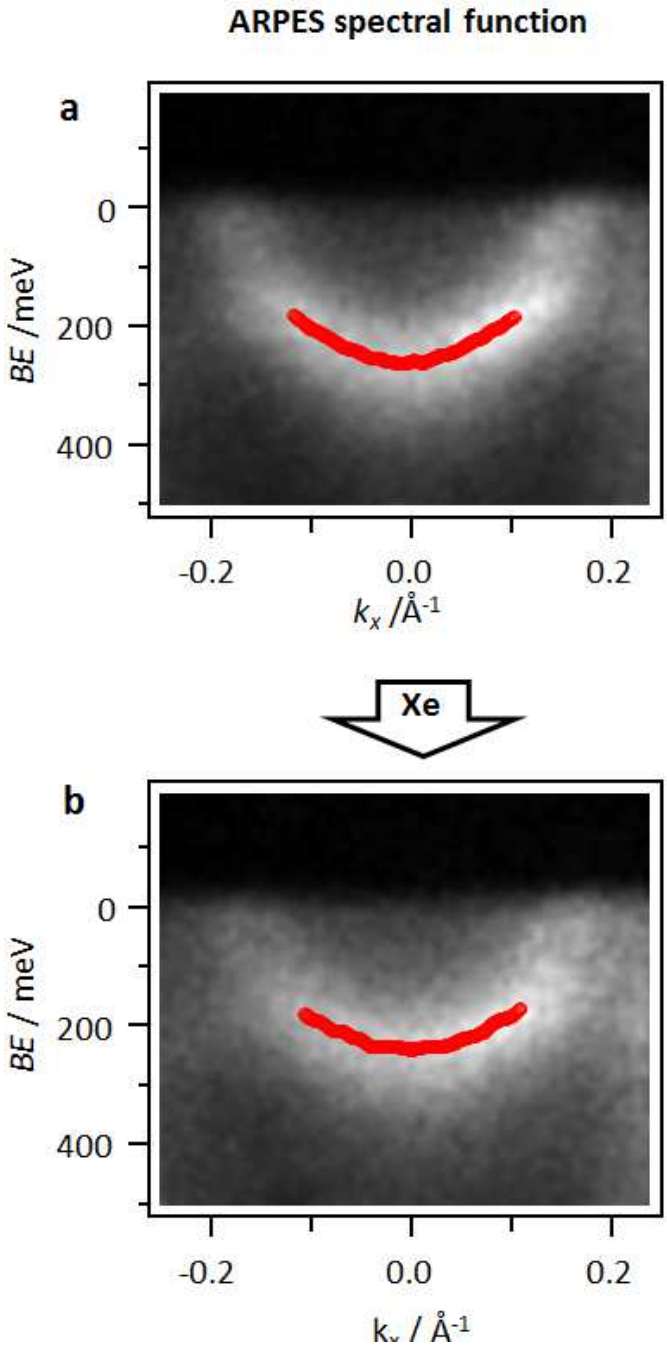

Figure 3. Apparent effective mass change after Xe pore adsorption. ARPES spectral function of the surface state region (a) before (black line in Figure S1c) and (b) after (blue line in Figure S1c) the Xe adsorption in the pores of the Cu-coordinated 3deh-DPDI network on Cu(111). The data were fit using a single convoluted Lorentzian-Gaussian component on a linear background and multiplied by a Fermi-Dirac distribution. The red line indicates the energy position of the component whose Gaussian width has been fixed to 0.1 eV to account for instrumental broadening, while the Lorentzian was left free, yielding an average increase of 0.12 to 0.14 eV with Xe presence. An upward energy shift of the minimum energy and a reduction of the band dispersion are observed when Xe is adsorbed in the pores. Using a parabolic fit to each we extract an apparent increase of the effective mass from a m^*/m_0 = 0.57±0.02 to b m^*/m_0 = 0.66±0.02.

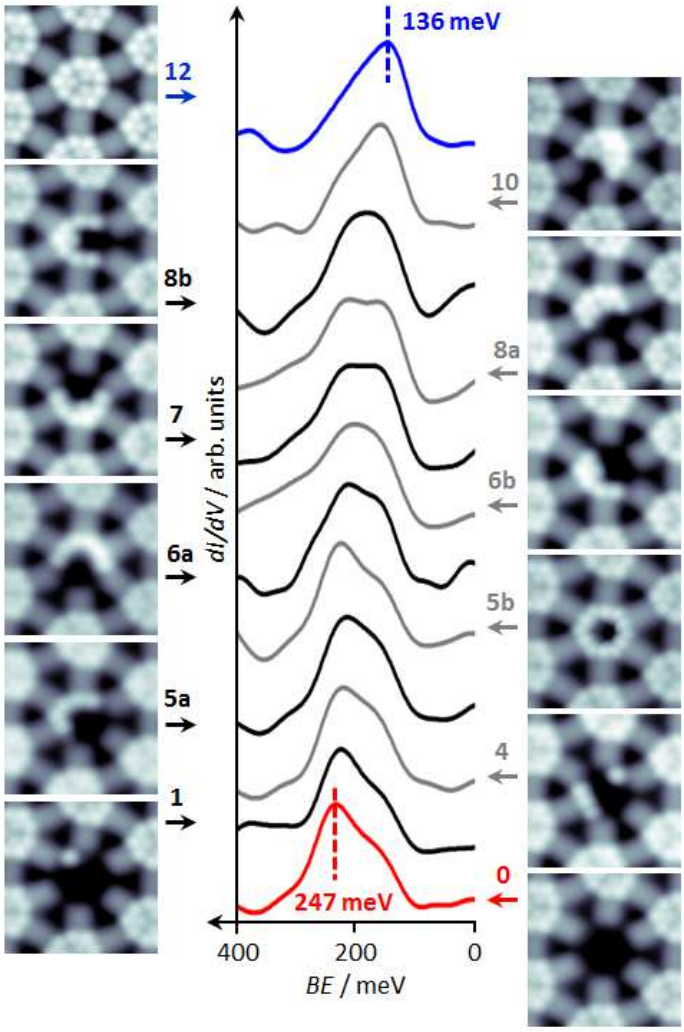

Figure 4. Influence of the Xe occupancy in one particular quantum box on the electronic state. d*I*/d*V* spectra and the corresponding STM images (4 nm x 4 nm) acquired for pores hosting different numbers of Xe atoms contained in the central quantum box surrounded by filled ones. The numbers and letters above the arrows indicate the amount and arrangement of Xe within the central pore. The d*I*/d*V* spectra were acquired above the Xe-free area within the pore of the corresponding quantum boxes, except for the quantum box filled with 12 Xe atoms, in which case the d*I*/d*V* spectrum was measured above the pore center. All occupancies were created by removing Xe atoms from the central quantum box initially filled with 12 Xe.

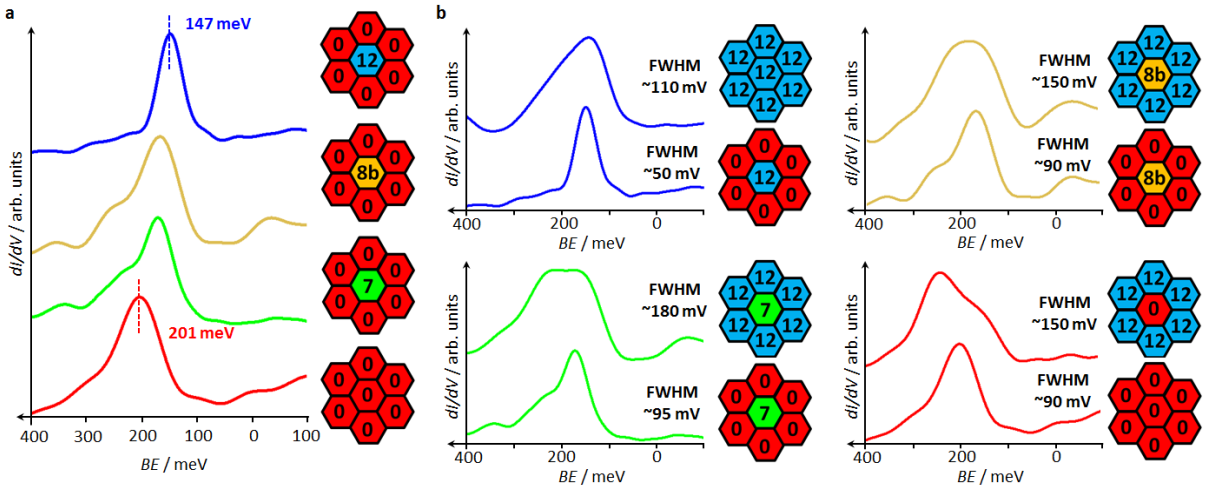

Figure 5. Influence of the number of Xe atoms adsorbed in a central QB and the influence of the filling level of the surrounding ones on the quantum box state (a) The influence of the number of Xe contained in a central QB with the surrounding QBs empty. With decreasing occupancy a gradual shift of the electronic state is observed to higher BEs (like in the case of surrounding QBs filled cf. Figure 4). (b) Comparison of the d*I*/d*V* spectra acquired in the QB featuring the same Xe occupancy surrounded by all empty and all filled QBs. Upon filling of the surrounding pores with Xe the spectral distribution of the quantum box state significantly changes.

Table 1. Band structure parameters extracted from ARPES measurements

Sample	BE_{max} at $\bar{\Gamma}$ [a)] [meV]	m^*/m_0 [b)]	Bandwidth [meV]
Cu(111)	434 ± 2 [d)]	0.43 ± 0.01 [d)]	-
Xe / Cu(111)	291 ± 2 [d)]	0.44 ± 0.02 [d)]	-
network [c)] / Cu(111)	270 ± 10	0.57 ± 0.02	90 ± 10
Xe / network [c)] / Cu(111)	240 ± 10	0.66 ± 0.02	70 ± 10

[a)] The values refer to the binding energy at normal emission (band bottom); [b)] the effective mass and the bandwidth of the n=1 state along $\bar{\Gamma}\ \bar{M}$; The details of extracting the effective mass from the ARPES spectral functions before and after filling of the pores with Xe can be found in Figure 3. [c)] 'Network' here denotes the Cu-coordinated 3deh-DPDI network formed on Cu(111); [d)] Values from Ref. [23].

A 2D array of electronically coupled quantum boxes is fabricated by means of on-surface self-assembly assuring ultimate precision of each box. The quantum states embedded in the boxes are configured by adsorbates, whose occupancy is controlled with atomic precision. The electronic inter-box coupling can be maintained or significantly reduced by proper arrangement of empty and filled boxes.

Keywords quantum box, electron confinement, surface state, scanning tunneling spectroscopy (STS), angle-resolved photoemission spectroscopy (ARPES)

S. Nowakowska,* A. Wäckerlin, I. Piquero-Zulaica, J. Nowakowski, S. Kawai, C. Wäckerlin, M. Matena, T. Nijs, S. Fatayer, O. Popova, A. Ahsan, S. F. Mousavi, T. Ivas, E. Meyer, M. Stöhr, J. E. Ortega, J. Björk, L. H. Gade,* J. Lobo-Checa,* T. A. Jung*
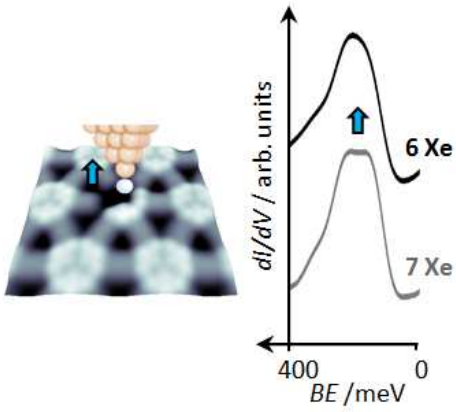
Configuring Electronic States in an Atomically Precise Array of Quantum Boxes